

The X/Ka Celestial Reference Frame: towards a GAIA frame tie

C. García-Miró*, I. Sotuela

Madrid Deep Space Communications Complex/NASA, INTA/ISDEFE, Spain
E-mail: cgmiro@mdscc.nasa.gov

C.S. Jacobs, J.E. Clark, C.J. Naudet, L. A. White

Jet Propulsion Laboratory, California Institute of Technology/NASA, USA

R. Madde¹, M. Mercolino¹, D. Pazos²

¹ESOC, ESA, Germany; ²Telespazio, Argentina

G. Bourda, P. Charlot

Laboratoire d'Astrophysique de Bordeaux, France

S. Horiuchi, P. Pope

Canberra Deep Space Communications Complex/NASA, CSIRO, Australia

L.G. Snedeker

Goldstone Deep Space Communications Complex/NASA, SaiTech, USA

An X/Ka-band (8.4/32 GHz) celestial reference frame has been constructed using single baselines from the combined NASA and ESA Deep Space Networks for approximately 100 sessions each of ~24-hour duration. The frame solution has dramatically improved with respect to the last reported frame due to the inclusion of Southern NASA-ESA baselines, routine 2-Gbps data rates, and correction of instrumental delays by recently deployed Ka-band phase calibration tones.

Comparisons with the S/X-band (2.3/8.4 GHz) ICRF-2 reference frame will be presented showing increasing agreement for 525 common sources. About 135 sources are located in the south polar cap ($\delta < -45^\circ$) which became accessible for first time with the addition of the ESA station in Malargüe, Argentina to our project's network. There is evidence for systematic errors at the 100 μs level. The known sources of error will be discussed.

Frame tie precision with Gaia has been estimated in about $\pm 7 \mu\text{s}$ (1- σ , per 3-D rotation component) using measured X/Ka position uncertainties and simulated Gaia uncertainties. Compared to X-band, Ka-band allows access to more compact radio source morphology and reduced core shift which should reduce these systematic errors compared to a tie of Gaia to S/X-band VLBI. However, there is a great deal of uncertainty in the offset between optical and radio centroids from effects such as optical host galaxy asymmetry which may ultimately limit the frame tie accuracy.

Acknowledgements: Research done in part under NASA contract. Sponsorship by U.S. Government, and our respective institutes acknowledged. Copyright ©2015. All Rights Reserved.

*12th European VLBI Network Symposium and Users Meeting,
7-10 October 2014
Cagliari, Italy*

1. Introduction

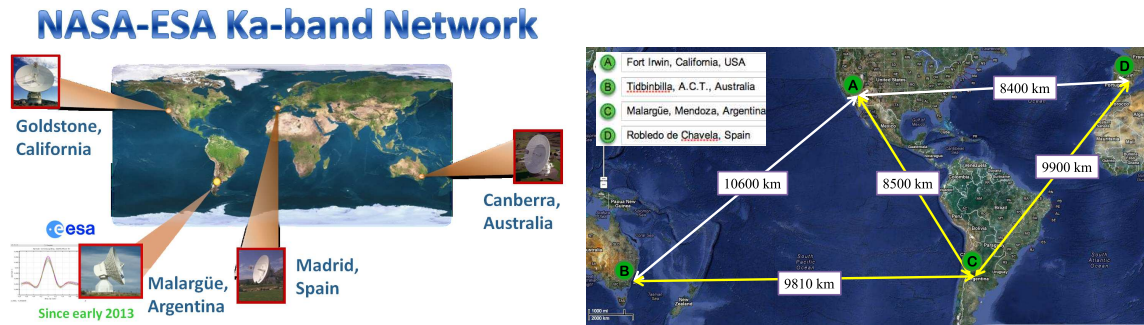


Figure 1: NASA-ESA combined Ka-band network: southern geometry is greatly aided by addition of Argentina (left) providing 3 more baselines and full sky coverage (right).

The NASA’s Deep Space Network (DSN) is the largest and most sensitive scientific communications system in the world and during 2014 reached its 50th anniversary. This international array of giant radio antennas supports interplanetary spacecraft missions, plus a few that orbit Earth. The DSN also performs radar and radio astronomy observations that improve our understanding of the solar system and the universe. Additionally motivated by the need to navigate inter-planetary space probes, the DSN also constructs VLBI radio reference frames to measure spacecraft positions and motions. Moreover, the DSN is an excellent instrument for astrometric measurements due to its large apertures, low system temperatures, high data rates and long baselines (> 8000 km).

However, the DSN’s single southern site limits the southernmost observed declinations ($> -45^\circ$). To overcome this deficiency, a collaboration with the European Space Agency’s (ESA) 35-m antenna located in Malargüe, Argentina (Fig. 1) was initiated, thereby adding three more baselines to the DSN’s two baselines. We note the near perpendicular mid-latitude baselines (California-Australia and California-Argentina) and the all-southern baseline (Australia-Argentina) which completed full sky coverage by giving Ka-band access to the south polar cap for first time.

Higher data rate requirements for spacecraft telemetry and the need of smaller and lighter radio frequency systems in the spacecraft are driving the DSN to higher frequencies, from X to Ka-band (32 GHz). The radio catalog presented in this paper was realized at X/Ka band due to spacecraft needs. Fortunately, Ka-band offers the advantage of reduced astrophysical systematic errors from reduced core shift and from accessing more compact source morphology.

We note that international Ka-band acceptance is growing. About 20 antennas around the world have, will have, or are considering acquiring 32 GHz capability. Jacobs *et al.* (2012 [7]) discuss the potential for a worldwide Ka-band VLBI network capable of high resolution imaging and astrometry of the most compact regions in Active Galactic Nuclei.

This paper is organized as follows: Section 2 describes the nature of the astrometric targets and the role of the observed frequency, Section 3 presents the X/Ka-band Celestial Reference Frame and compares it with current radio-based celestial frames, Section 4 discusses the viability of a frame tie between the Gaia optical frame and the DSN X/Ka radio frame.

*Speaker.

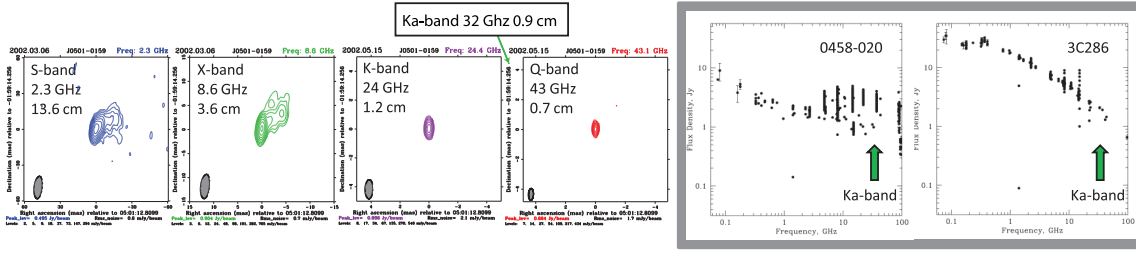


Figure 2: Nature of astrometric targets. **Left.** Source structure and compactness vs. wavelength for 0458-020 (Pushkarev & Kovalev 2012 [17], Charlot *et al.* 2010 [3]). **Right.** Multi-epoch radio spectrum for 2 different astrometric sources: 0458-020 and 3C286 (MOJAVE project, Lister *et al.*, 2009 [10]).

2. Astrometry at Higher Radio Frequencies

A perfect astrometric target would be a point source at infinity. While no radio source meets this ideal, the cores of quasars and radio galaxies can approach this standard. Typically for self-absorbed synchrotron sources, the observed flux density distribution on VLBI scales becomes more compact but weaker at higher observing frequencies (Fig. 2; König, 1981 [8]).

Recent efforts at higher frequencies are beginning to provide very promising astrometric results (Lanyi *et al.* 2010 [9], Charlot *et al.* 2010 [3]). Our Ka-band (32 GHz) observations, approximately a factor of four larger than the usual X-band, also take advantage of the more compact structure of the targets apart from avoiding the S-band Radio Frequency Interference (RFI) and reducing the ionosphere and solar plasma effects on group delay and signal coherence by a factor of ~ 15 allowing observations closer to the Sun and the Galactic Center.

The increase in frequency also implies several disadvantages. Moving closer to the water vapor line at 22 GHz increases the system temperature to up to 10–15 K per atmosphere or more, thereby greatly increasing vulnerability to poor weather. Furthermore, the sources themselves are in general weaker and many sources are resolved, with therefore less sources detectable. Also, the coherence times are shortened so that practical integration times are a few minutes or less and lastly the antenna pointing accuracy requirements must be tightened by the same factor of four. The combined effect of these disadvantages reduces the system sensitivity. Fortunately, recent advances in recording technology (e.g. García-Miró *et al.*, 2015 [5]) make it feasible and affordable to offset these losses in sensitivity by recording at higher data rates.

3. The X/Ka-band Celestial Reference Frame

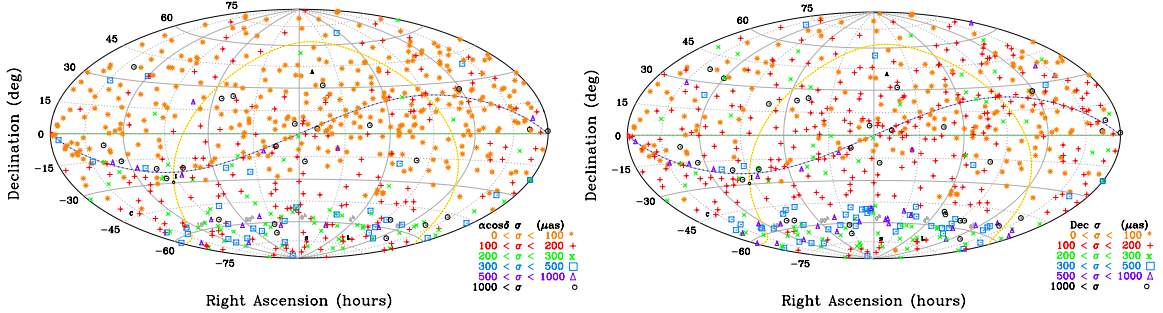
The results presented here are from approximately 100 Very Long Baseline Interferometry (VLBI) observing sessions of ~ 24 hour duration (35,000 group delay/phase rate observations) performed from July 2005 until September 2014 using NASA’s stations in Goldstone (California), Tidbinbilla (Australia) and Madrid (Spain), and since early 2013, the ESA station located in Malargüe, Argentina. Jacobs *et al.* (2011 [6]) give details on the experiment design and analysis.

We have detected 654 extragalactic radio sources with full sky coverage, of which 138 are located in the south polar cap made accessible for first time due to the ESA site in Argentina. The

new south polar cap sources were selected from Petrov (RFC2011 [15]) when fluxes $>200\text{mJy}$ and 70% of its total flux was unresolved. We detected 96% of our candidates. Fig. 3 shows the location in the sky of the X/Ka catalog sources using a Hammer-Aitoff projection.

Comparisons with the S/X-based (2.3/8.4 GHz) ICRF-2 reference frame (Ma *et al.* 2009 [13]) show improving agreement for the 525 common sources. For these sources, the weighted RMS (wRMS) differences are $\sim 165\ \mu\text{as}$ in $\alpha \cos \delta$ and $\sim 205\ \mu\text{as}$ in δ . When comparing with a recent 2014 Goddard solution (GSFC-2014bp3, Gordon *et al.*, private comm., NASA Goddard, 2014) the wRMS slightly improves to 154 and 195 μas in $\alpha \cos \delta$ and δ , respectively. Moreover the declination bias decreases from -102 to -60 μas , showing a significant reduction of systematic errors between the frames.

Systematic errors at the 100 μas level include limited SNR, partially calibrated instrumentation, and tropospheric turbulence. Recently we increased the data rate by factor of 4 to 2 Gbps using a new DSN digital backend (García-Miró *et al.*, 2015 [5]). Ka-band phase calibrators have been installed at Goldstone with units being prepared for Canberra and Madrid. Water vapor radiometer calibrations have been demonstrated, but are available only at some antennas.



3a. RA* (arc) precision: Median σ is 96 μas . Note lower precision for Dec $< -45^\circ$ because less than 5% of data is from the all-southern baseline.

3b. Dec precision: Median σ is 126 μas . Note lower precision for Dec $< -45^\circ$ because less than 5% of data is from the all-southern baseline.

Figure 3: Distribution of 654 X/Ka sources plotted using a Hammer-Aitoff projection to show their locations on the sky. $\alpha = 0$ is at the center. The ecliptic plane is shown by the dashed blue-gray line and the Galactic plane is indicated by the yellow-red dashed line. The sources are color and symbol coded according to their 1- σ formal $\alpha \cos \delta$ and δ uncertainties with the value ranges indicated in the legend.

4. Gaia Optical Frame Tie

The ESA's Gaia astrometric observatory was launched December 19th 2013. It scans the sky using twin telescopes with the aim to observe 10^9 objects down to $V = 20$ visual magnitude (500–600 nm), including 500,000+ quasars of which about 2,000 quasars should be radio loud (30–300+ mJy) and optically bright ($V < 18$ mag). Position precision will range from 25 μas at $V = 16$ to $\sim 70\ \mu\text{as}$ at $V = 18$. Several issues with Gaia performance may affect accuracies for $V \geq 18$ objects.

The Gaia optical frame (Lindgren *et al.*, 2008 [11]) will also use quasars as defining sources thus allowing direct comparison with VLBI, starting with the release of the position-only First Notional Intermediate catalog in mid-2016. Bourda *et al.* (2012 [2]) found that only 6% of the

ICRF-2 sources (195) are bright ($V \leq 18$) and compact enough to make significant contributions to an optical-radio tie. The sample for potential Gaia tie sources has therefore been enhanced by adding 119 sources selected from a sample of 447 optically bright ($V \leq 18$) extragalactic radio sources from the NRAO VLA Sky Survey (Bourda *et al.* 2010, 2011 [1]). These new Gaia tie sources, mostly located in the Northern Hemisphere, were included in our DSN S/X catalog (Fig. 4, left), and 18 of them, the strongest flat spectrum sources, were also detected in X/Ka. Fig. 4b. (right) shows optical magnitudes for the X/Ka sources (Veron-Cetty & Veron, 2010 [18]) with 345 sources having optical counterparts bright enough to be detected by Gaia ($V < 20$ mag) and 175+ objects having optically bright counterparts ($V < 18$).

Using existing X/Ka-band uncertainties and simulated Gaia uncertainties (Gaia, (2012 [4]) *corrected for ecliptic latitude, but not V–I color*), a covariance study predicts that the X/Ka and Gaia frames could be aligned with a precision of $\sim 7 \mu\text{as}$ per 3-D rotation angle ($1-\sigma$), a number so small that one must expect systematic errors to dominate the true accuracy.

Therefore, a tie between the optical and radio frames requires a deep understanding of the different emitting regions in relativistic jets. In the radio regime, increasing frequency tends to more compact but weaker sources. Moreover, opacity effects due to synchrotron self-absorption, that alter the core position, are greatly reduced at higher frequencies. This core shift for phase delay from X to Ka is expected to be $\sim 100 \mu\text{as}$ and from Ka to optical $\sim 25 \mu\text{as}$. However, Porcas (2009 [16]) argues that, under minimum energy conditions or (near) equi-partition of particle and magnetic energy in the jets (Pacholczyk, 1970 [14]), the effect on the group delays used on radio frames is several times smaller than on phase delay.

With respect to the radio-optical centroid offset, for radio-loud quasars the optical and radio emission may both be dominated by the emission from the jet (subjected to opacity effects) while for radio-quiet quasars the optical emission is dominated by the non-thermal emission from a central ionizing source (corona or wind) and the thermal component from the accretion disk ("big blue bump"), while radio emission from the jet is weak or absent (Wehrle *et al.*, 2009 [19]). Given Gaia's ~ 60 mas linear spread function (Mignard 2014, private comm.), asymmetry from the host galaxy may bias the optical centroid. Zacharias & Zacharias (2014 [20]) estimate that these biases may be many *mas* or even larger which would dominate the tie error budget.

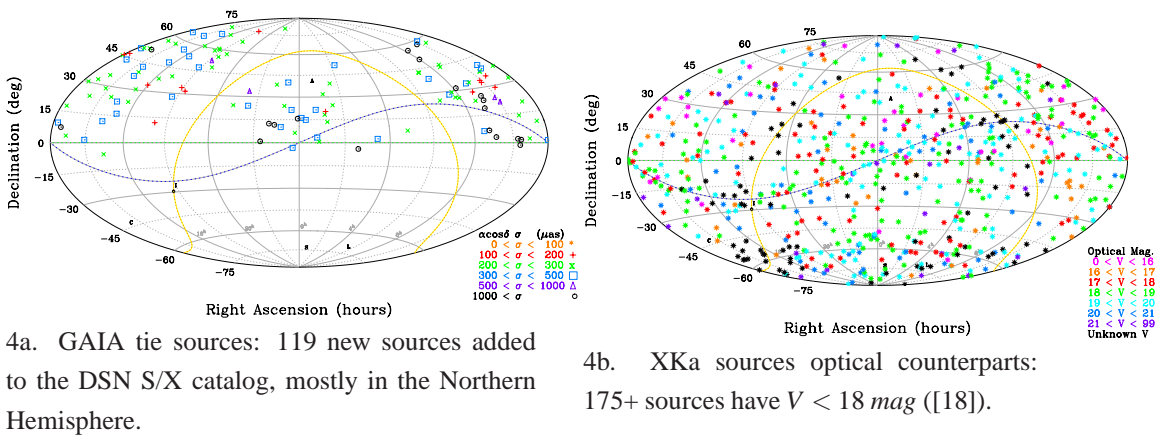


Figure 4: X/Ka Radio Frame to Gaia Optical Frame tie

5. Conclusions

The ESA-NASA collaboration has greatly improved our X/Ka network configuration, achieving full sky coverage by accessing the south polar cap for the first time. Astrometric results are improving rapidly due to this augmented geometry, the improved astrophysical stability at 32 GHz, increased data rates (2 Gbps), and Ka-band instrumental calibrators. Comparison of 35,000 group delay/phase rate observations at X/Ka with the S/X-based ICRF-2 reference frame shows agreement below 200 μas (1 nrad) in both axes. Declination bias is a concern, but recent S/X solutions reduce the absolute value of the bias to 60 μas . In order to achieve true accuracy better than 100 μas , we need to reduce systematic errors with further observations using ESA's Malargüe antenna and any other Ka-band worldwide antennas, installation of Ka-band instrumental phase calibrators at all DSN sites, and usage of water vapor radiometers to calibrate the troposphere. These results give hope that better than 100 μas radio accuracy might be achieved in the near future. If optical systematics can be calibrated with comparable accuracy, a new era in reference frame alignment will be born.

References

- [1] G. Bourda, et al., *VLBI obs. for alignment with future Gaia frame:I & II*, *A&A*, 520, 2010; 526, 2011
- [2] G. Bourda, et al., *Towards Accurate Alignment with Future Gaia Optical Frame.*, *IVS GM*, 2012.
- [3] P. Charlot, et al., *CRF at 24 & 43 GHz II. Imaging*, *AJ*, 139, 2010.
- [4] Gaia, http://www.rssd.esa.int/index.php?project=GAIA&page=Science_Performance, 2012.
- [5] C. García-Miró, et al., *VLBI digital terminal at the DSN* in proc. of *12th EVN Symposium*, 2015.
- [6] C.S. Jacobs, et al., *XKa CRF*, in proc. *20th EVGA*, 166, 2011.
- [7] C.S. Jacobs, et al., *Ka-band Worldwide VLBI Network* in proc. of *IVS GM*, 2012.
- [8] A. Konigl, *Relativistic Jets as X-ray and gamma-ray Sources*, *ApJ*, 243, 700, 1981.
- [9] G. Lanyi, et al., *CRF at 24 & 43 GHz I. Astrometry*, *AJ*, 139, 2010.
- [10] M. Lister, et al., *MOJAVE*, *AJ*, 137, 2009.
- [11] Lindegren, et al., *Gaia Mission*, in proc. *IAU 248*, 217, 2008.
- [12] Lindegren, et al., *The astrometric core solution for the Gaia mission*, *A&A*, 538, 2012.
- [13] C. Ma, et al., *2nd Realization of ICRF by VLBI*, *IERS Tech Note 35*, 2009.
- [14] A. G. Pacholczyk, *Radio Astrophysics*, W.H. Freeman, 1970.
- [15] L. Petrov, *The Catalog of Positions of OBRS-I*, *AJ*, 142, 2011.
- [16] R.W. Porcas, *Radio Astrometry with Chromatic AGN Core Positions*, *A&A*, 505, 2009.
- [17] A.B. Pushkarev & Y.Y. Kovalev, *VLBI imaging of bright AGN at 2 and 8 GHz*, *A&A*, 544, 2012.
- [18] Veron-Cetty & Veron, *Catalogue of quasars and active nuclei: 13th edition*, *A&A*, 51, 2010.
- [19] A. Wehrle, et al., *μas Science*, Socorro, 2009.
- [20] N. Zacharias, M.I. Zacharias, *Radio-Optical Reference Frame Link*, *AJ*, 147, 2014.